Design and qualification of an on-line permeator for the recovery of tritium from lead–lithium eutectic breeding alloy

G. Veredas [a], J. Fradera [b], I. Fernández [a], L. Batet [b], I. Peñalva [c], L. Mesquida [d], J. Abellà [d], J. Sempere [d], I. Martínez [e], B. Herrazti [e], L. Sedano [a]

[a] EURATOM-CIEMAT Fusion Assoc., Breeding Blanket Tech. Unit, Av. Complutense 22, E-28040, Madrid, Spain.
[b] Tech. Univ. of Catalonia (UPC), Department of Physics & Nuclear Engineering, Av. Diagonal 647, E-08028, Barcelona, Spain.
[c] UPV-EHU, Dept. of Nuclear Engineering and Fluid Mechanics, Alda. de Urquijo, E-48103, Bilbao, Spain.
[d] ETS Institut Quimic de Sarria, Universitat Ramon Llull, Via Augusta, 390, E-08017, Barcelona, Spain.
[e] SENER Ingeniería y Sistemas, Provenc¸ a 392, 4a, E-08025, Barcelona, Spain.

Abstract

The fast and efficient recovery of bred tritium represents a major milestone of tritium breeding technologies R&D and is key for the demonstration of fusion reactor fuel self-sufficiency. For lead–lithium eutectic, diverse technologies are currently being investigated and qualified. Permeator Against Vacuum (PAV) solution represents a firm candidate because: (i) runs as a single-step process for tritium on-line recovery, (ii) works passively allowing to be thermally governed, (iii) can be easily in-pipe integrated in Pb15.7Li loop systems and (iv) can be conceived with high compactness. An optimal design of a PAV requires a detailed hydraulic design optimization for established operational ranges. An optimal PAV design is proposed and qualified by numerical simulation.

Keywords

Tritium breeding; tritium self-sufficiency; tritium recovery, permeator.

1. Introduction

Tritium Plant Systems characteristic processing times tP are today (ITER reference) in the order of a few hours [1] (Fig. 1). Thus, the required tritium reactor starting inventory I01 guaranteeing the reactor fuel self-sufficiency

$$I_0 = H(t_R - t_p)\left[\frac{\dot{c}}{b}t_R - (1-b)\frac{\dot{c}}{b}(t_R - t_p)\right] + H(t_p - t_R)\left[\frac{\dot{c}}{b}t_p - TBR\dot{c}(t_p - t_R)\right] \quad (1)$$

will depend strongly on fuel burn-up fraction b and subsidiarily on the tritium residence time at breeding blanket systems t_R, residence time at breeding loop t_B plus the tritium characteristic processing times at Tritium Extraction Systems (TES) t_C (e.g., $t_R = t_B + t_C$). Typical fuel burn-up scenarios for ITER (and current DEMO) are b = 0.01, TBR < 1.18 and reference t_P values (hours) would mean tritium required starting inventories $I_0 \sim 30$ kg.

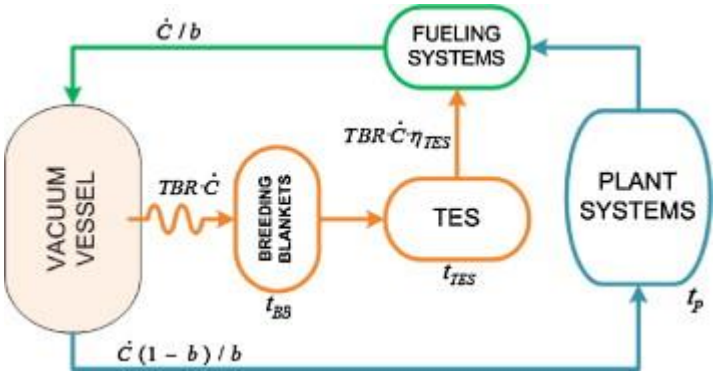

Fig. 1. Simplified lay-out for Plant Systems, tritium breeding blanket and extraction systems (TES) with characteristic times.

It should be kept in mind that under the most favourable tritium supply scenario, the ultimate civil tritium reserves for the next decade are about 27 kg [2]. It is planned that ITER will consume about 15 kg during its lifetime at the best operational conditions [1].

Therefore, with no dramatic improvements on burning plasma physics and/or tritium Plant Systems technologies in ITER, the pathway from ITER to future DEMO appears with major fuel supply concerns. Hence, the fuel self-sufficiency of future D-T reactors relies, not only on high breeding blanket performance (i.e., high TBR), but also on a more efficient plasma burn-up and on a faster bred tritium recovery (Fig. 2).

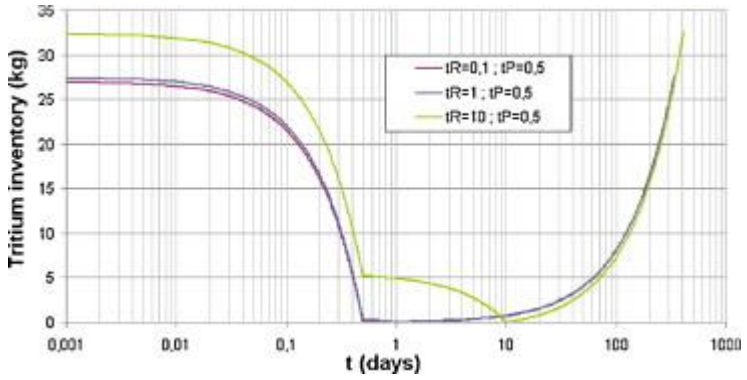

Fig. 2. Dependence of tritium required starting inventory on t_R for a 3450 MWth DEMO fusion reactor for different fractional burn-ups (assumed TBR=1.15, b=0.01 and t_p=0.5 day).

Therefore, it seems mandatory for the total bred tritium required processing times before availability for plasma refuelling t_R, to be much shorter (similar at most) than the reference t_P values.

t_B values are strongly dependent on (1) blanket design options, (2) tritium management strategies at breeding systems (e.g., consideration on whether permeation barriers are needed or not), and (3) choice of TES processing technologies.

Values of t_R have been assessed with specific Process Flow Diagrams developed at CIEMAT [3] by solving mass-balance equation 7×7 matrix for fluxes J_i and concentrations c_i (Fig. 3). Dual-Coolant Lead–Lithium (DCLL) breeding blankets [4], where tritium is bred in liquid metal flowing at tens of cm/s, the recovering requirement from ancillary He is minimized. DCLL appears as superior concept from tritium self-sufficiency because of minimizing t_B values (Fig. 4, Table 1).

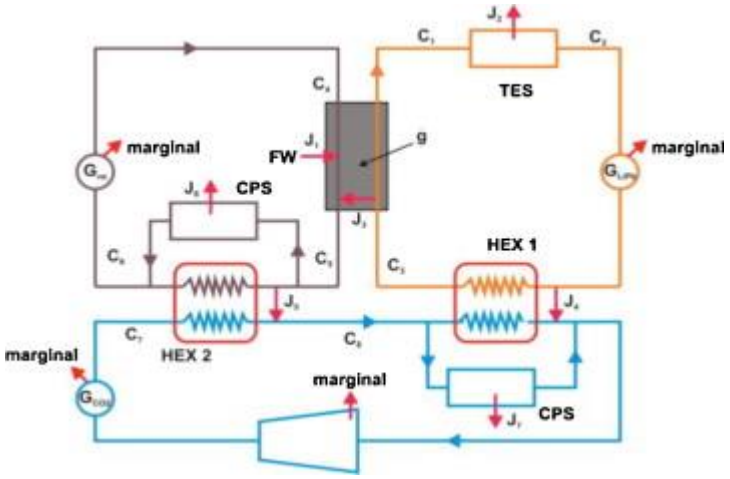

Fig. 3. Generic lay-out for He-cooled or He/Pb15.7Li dually cooled breeding blanket systems.

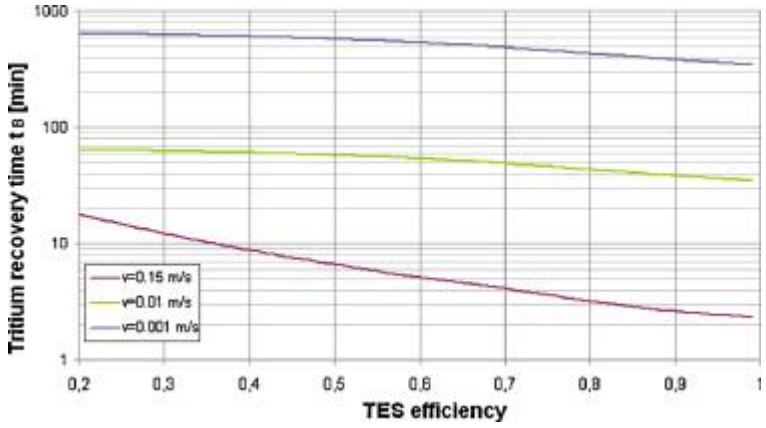

Fig. 4. Dependence of t_B given liquid metal flow rates (0.001 m/s in blue is a reference value for HCLL [3], and 0.15 m/s is the value for DCLL [4] breeding blanket design options). (For interpretation of the references to color in this figure legend, the reader is referred to the web version of this article.).

Table 1. Reference t_R values for diverse candidate TES [5].

TES technique	**t_R**
PB sweepers + TRS	~fraction of hours [6], [8]
PB strippers + TRS	~fraction of hours [7], [8]
Immersed getters	~hours [5]
Immersed PAV[a]	~a few tens of seconds

[a] assessed in Section 2.

2. Immersed PAVs

Tritium has a very low solubility in Pb15.7Li, which results in very large in-solution tritium partial pressures. This leads to a high permeation flux through a permeable membrane in contact with the liquid metal. A permeator can be immersed in Pb15.7Li pipes to operate as a one-step steady-state passive system. It can be geometrically designed to maximize the surface in contact with the liquid metal while keeping an adequate hydrodynamic profile, thus minimizing pressure drop.

An innovative PAV design following this premise is proposed. It consists on a double membrane rolled in a spiral shape which maximizes the specific surface in contact with the flowing Pb15.7Li and hydrodynamics.

Multiple objectives are accomplished with this design: (1) *Highest contact surface*. Spiral rolled layout has the highest contact surface per unit of length. (2) *Hydrodynamics control*. Pb15.7Li flows between two close membranes. Separation of these membranes and an adequate surface finishing can induce the desired flow regime. An optimized geometric design can provide such conditions. (3) *Flow distribution.* The tips of the inner membrane can be curved to distribute the incoming flow equally. Also, the border of the double membrane can be rounded to make it more hydrodynamic and minimize pressure drop. (4) *Simplicity of manufacture*. Spiral rolling of a double membrane is an easy operation that does not require neither a difficult process nor expensive machinery. Membrane bending can be avoided by inserting rigid corrugated spacers, as seen in Fig. 5.

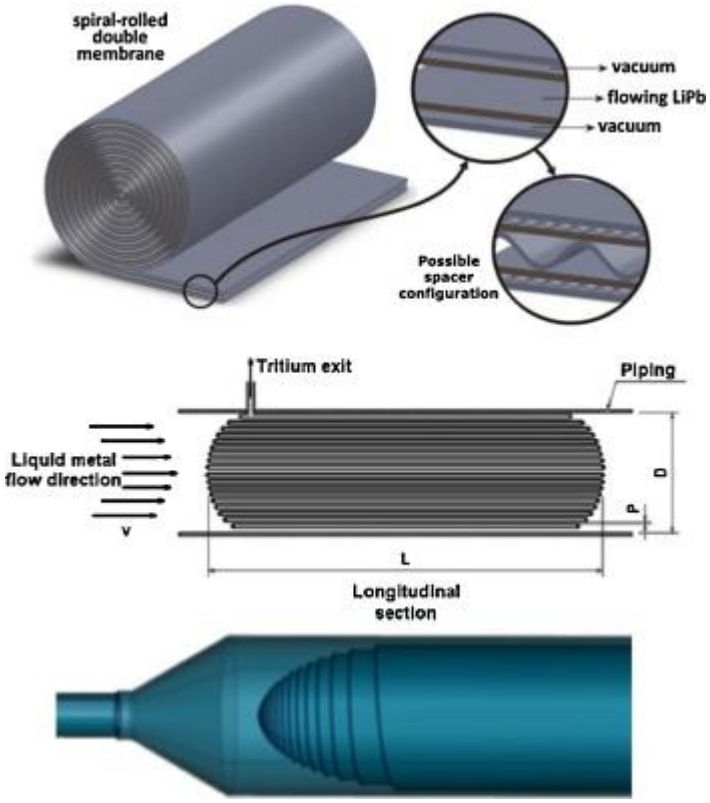

Fig. 5. Fuskite® [14] spiral-rolled double membrane concept and design of an in-pipe immersed PAV.

The optimal membrane and permeator materials should be chosen accordingly to various considerations. An ideal permeator membrane should show: (1) highest permeability at lower solubility, i.e., highest tritium diffusivity, (2) good compatibility with Pb15.7Li: low corrosion rates in flowing Pb15.7Li, (3) good concave wetting and (4) low oxidation potential when immersed in Pb15.7Li.

A good candidate material is α-Fe [6]. It has the highest tritium diffusivity and good compatibility behaviour in contact with Pb15.7Li, but careful preventive actions should be adopted to use clean material and avoid material oxidation. Additionally, a PAV allows active control of tritium permeability (then efficiencies) through wall temperature control by heating.

2.1. PAV finite differences and CFD efficiency assessment

Assuming steady-state, the microscopic mass balance in a differential radial volume of the membrane reads,

$$\frac{1}{r}\frac{dC}{dr}\left[r\frac{dC}{dr}\right]=0 \tag{2}$$

With the following boundary conditions:

$$\begin{Bmatrix} r=r_1 & C(r)=C(r_1) \\ r=r_2 & C(r)=C(r_1) \end{Bmatrix} \tag{3}$$

After integration the concentration profile is found.

$$\frac{C(r)-C(r_2)}{C(r_1)-C(r_2)}=\frac{ln\left({}^{r}/_{r_2}\right)}{ln\left({}^{r_1}/_{r_2}\right)} \tag{4}$$

The molar flux through the membrane wall facing the LM can be expressed as follows:

$$J=-D_T\frac{dC}{dr} \tag{5}$$

Therefore, the molar rate reads,

$$S=-2\pi rLD_T\frac{dC}{dr} \tag{6}$$

$$C_{T,LM}k_{s,T-m}=C_{T,SM}k_{s,T-m} \tag{7}$$

Substituting the concentration profile in the molar rate expression and assuming equilibrium through the solubility ratios, an expression for the molar rate is found:

$$S=-2\pi LD_T\frac{C(r_1)-\left(k_{s,T-LM}/k_{s,T-SM}\right)C(r_2)}{ln(r_1/r_2)} \tag{8}$$

The overall mass transfer coefficient including mass transfer resistance at the LM-m Km and the resistance due to the membrane thickness can be expressed as follows:

$$\frac{1}{k_T}=\frac{1}{k_m}+\frac{ln(r_1/r_2)}{2\pi LD_T} \tag{9}$$

Combining previous equations an expression for the molar rate per length of permeator is found.

$$S=-2\pi LD_T\frac{C(r_1)-\left(k_{s,T-LM}/k_{s,T-SM}\right)C(r_2)}{1/k_m+ln(r_1/r_2)/2\pi LD_T} \tag{10}$$

Mass transfer coefficient k_m has been suggested to be expressed through the following correlation from Harriott et al. [9]: $k_m = 0.0096\mathrm{Re}^{0.913}\mathrm{Sc}^{0.346}D_T/d$, where d is the channel diameter, Re and Sc are the Reynolds and Schmidt dimensionless numbers. Even under laminar flow, tritium is effectively removed.

A preliminary analysis of the permeator design, together with a simplified CFD simulation is tentatively done hereafter. A simplified CFD model has been developed and set up. In a preliminary approach a representative simplified axis-symmetric 3D domain is needed in order to save computational time. However, the actual design of permeator has a spiral cross section, making impossible to represent it with an axis-symmetric 3D domain. Therefore, the domain is represented by a series of concentric annular channels.

The permeator analysis presented assumes cylindrical coordinates and an inlet velocity of 1 mm/s (laminar case) or 10 cm/s (turbulent case), a channel height of 5 mm and a tube length of 2 m. In the present work a 2 m long permeator with 45 concentric channels has been chosen for the CFD simulations. Membrane thickness is set to 1 mm with a vacuum space of 1 mm. Channels are 5 mm thick [10].

For the permeator design efficiency assessment it is crucial to model mass transfer mechanisms under turbulent flow driving to h_m mass-exchange coefficient values in the range of 10^{-3} m/s [9]. In the laminar regime (Re ~ 65, $h_m \sim 10^{-6}$ m/s), a PAV would be driven by tritium residence time. Concentration in the bulk liquid is extracted in each channel asymmetrically, due to the bigger surface area of the external wall with respect to the internal one (Fig. 6) where *T* concentration decreases much faster. The same effect is observed for all the channels. The overall tritium molar rate to the permeable surface is $\sim 10^{-6}$ mol/s, which is also in well agreement with the non-limiting boundary condition.

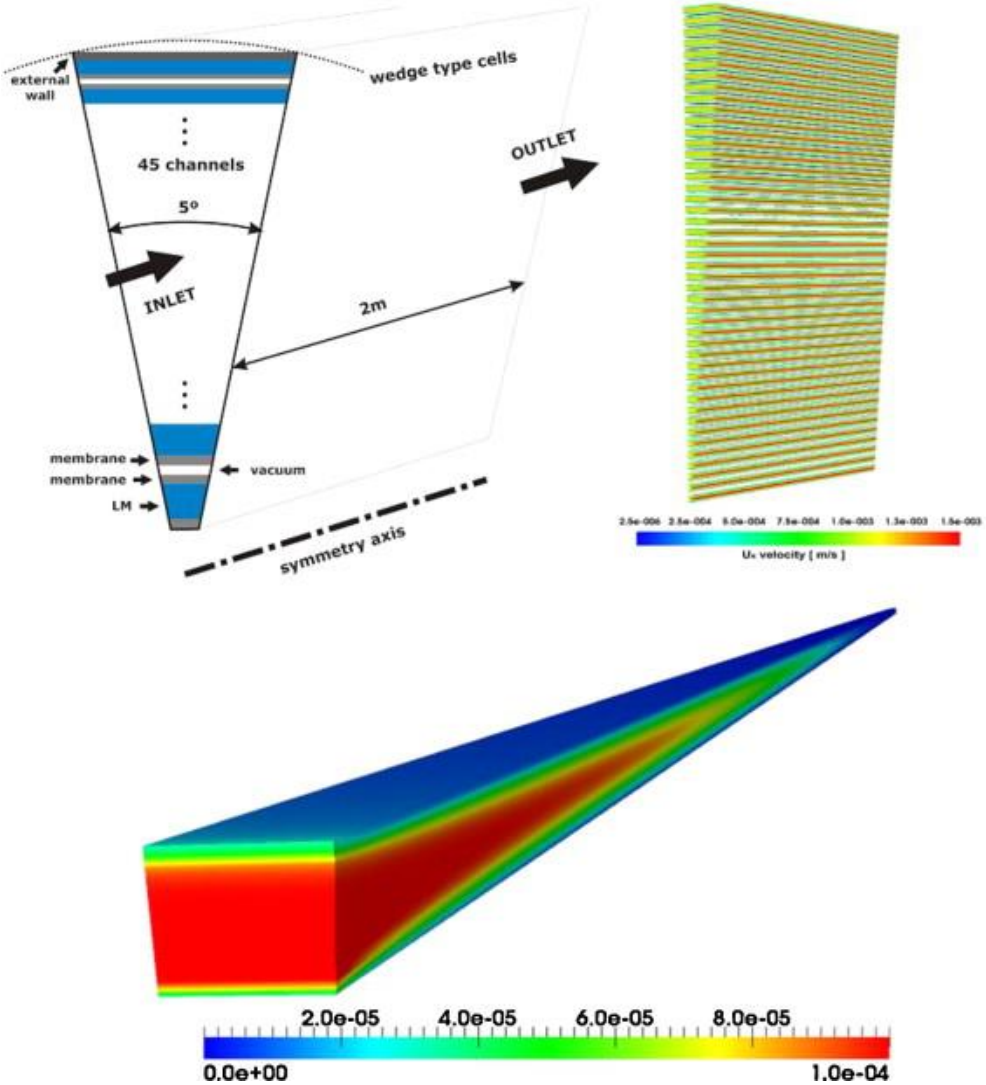

Fig. 6. FVM efficiency assessment under laminar regimes. Top/left: channel geometric simplifications; top/right and bottom: tritiujm concentration (mol/s·m^3) evolution along channels [10].

At high velocities the flow regime inside the permeator channels is turbulent. Liquid metals have a high specific heat conductivity (low Prandtl numbers) which yields in numerical simulations to many problems, since the viscous and the thermal length scales separate. In the present work a *k*–*ω* SST is used because it is formulated for low Reynolds numbers. *k*–*ω* SST gives good results and realistic boundary layer velocity distributions (see Gordeev et al. [11]), however, other models like the TMBF (Lefhalm et al. [12]) are known to give better results for liquid metals (Carteciano [13]). Channel number 15 of the rolled permeator has been simulated for an inlet

velocity of 1 m/s with a laminar solver and the k–ω SST model. Laminar solver does not reach the steady state, but reaches an oscillatory regime. On the contrary, turbulent solver reaches the steady state. Velocity profiles at x = 1 m are shown in Fig. 7.

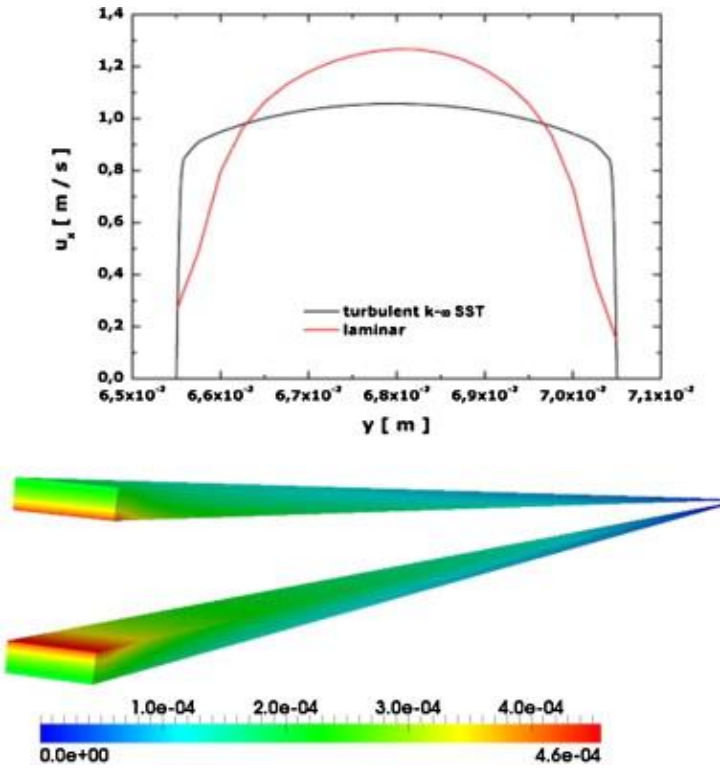

Fig. 7. FVM efficiency assessment under turbulent regimes. Top: comparison between tritium concentration along channels in developed velocity profiles; bottom: tritium concentration (mol/s m^3) evolution along channels [10].

2.2. Application to DEMO HCLL and DCLL

Under optimizations, a PAV can achieve a very high efficiency (>0.9). Typical residence times for high velocity options are in the order of minutes; e.g., laminar regimes and less than few tens of seconds in turbulent ones. In a HCLL TBM, Pb15.7Li flows at low velocity (1 mm/s). Under these conditions, a high efficiency can be achieved even at reduced pipe diameters. Again, efficiency was calculated for 10 cm/s flow, using typical parameters. As it can be seen in Fig. 8, we need about 1 m of permeator length for a Ø0.5 m pipe and 99% efficiency.

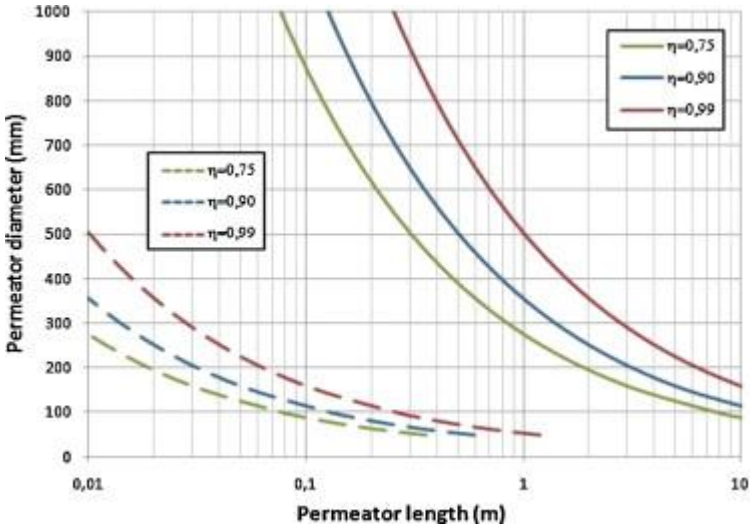

Fig. 8. Efficiency assessment for HCLL [3] and DCLL [4].

3. Conclusions

Taking into account the residence times of tritium plant processing systems in ITER and tritium availability for the first generation of DT DEMO reactors, PAV represents the simplest, cost effective and reliable technology to be qualified for tritium recovery from liquid-metal breeders. An advanced design of PAV (Fuskite®) has been proposed together with a preliminary numerical qualification of its recovery efficiency at HCLL and DCLL [4] loop scale. The results show the technical attractiveness of PAVs as tritium processing solution for liquid metal breeding blankets. PAV manufacturing has been demonstrated according to initial design specifications. Experiments for prototype qualification are ongoing (Fig. 9).

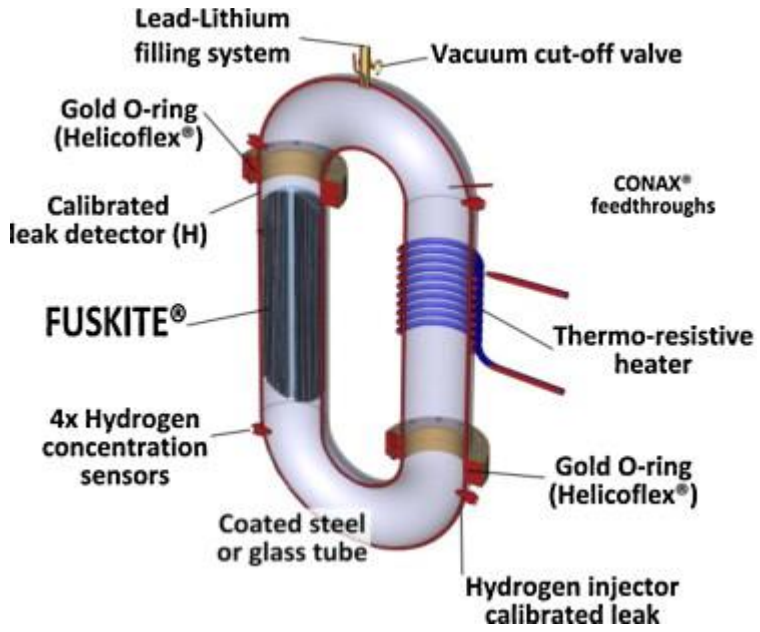

Fig. 9. Design of a prototyping qualification loop for Fuskite® design [14].

Acknowledgements

This work is funded by the Spanish National Project on Breeding Blanket Technologies TECNO_FUS through CONSOLIDER-INGENIO 2010 Programme.

References

[1] I.R. Cristescu, et al., Tritium inventories and tritium safety design principles for the fuel cycle of ITER, Nuclear Fusion, 47 (2007), pp. 458-463.

[2] M. Abdou, Keynote Presentation at ISFNT7, Tokyo, Japan, (2005).

[3] L. Sedano, et al., Inner breeding tritium cycle conceptual design and tritium control strategies for HCLL blankets, in: 24th SOFT, 11–15 September, Warsaw, Poland.

[4] P. Norajitra, et al., Conceptual design of the dual-coolant blanket within the framework of the EU power plant conceptual study, FZKA 6780, May 2003.

[5] L. Sedano, Tritium cycle design for He-cooled blankets for DEMO, CIEMAT Internal Report 1110, June 2007.

[6] L. Sedano, Efficient recovery of tritium from Pb17Li using small extraction columns, EU 18147 EN, 1998.

[7] L. Kosek (NRI), Personal Communication.

[8] H. Albrecht, Tritium recovery from a solid breeder DEMO blanket, Transaction on Fusion Technology, 27 (1995).

[9] P. Harriott, R.M. Hamilton, Solid–liquid mass transfer in turbulent pipe flow, Chemical Engineering Science, 20 (12) (1965), pp. 1073-1078.

[10] J. Fradera, Preliminary study of a permeator for tritium extraction in nuclear fusion reactors, UPC/T4F/Greener Report T4F201001_01, Barcelona, 2009.

[11] S. Gordeev, L. Stoppel, R. Stieglitz, Turbulent liquid metal flow in rectangular shaped contraction nozzles for target applications, International Journal of Computational Fluid Dynamics, 23 (6) (2009), pp. 477-493.
[12] C.H. Lefhalm, N.I. Tak, H. Piecha, R. Stieglitz, Turbulent heavy liquid metal heat transfer along a heated rod in an annular cavity, Journal of Nuclear Materials, 335 (2) (2004), pp. 280-285.
[13] L.N. Carteciano, Entwicklung eines Turbulenzmodells für Auftriebsströmungen, Wissenschaftliche Berichte/FZK Karlsruhe, Germany, (1996).
[14] Fuskite®, Registered design, Patent pending.